Catalytic performance of cobalt–silica catalyst for Fischer–Tropsch synthesis

Moazami, Nima; Mahmoudi, Hamid; Rahbar, Kiyarash; Panahifar, Pooria; Tsolakis, Athanasios; Wyszynski, Miroslaw L

DOI:
10.1016/j.ces.2015.05.025

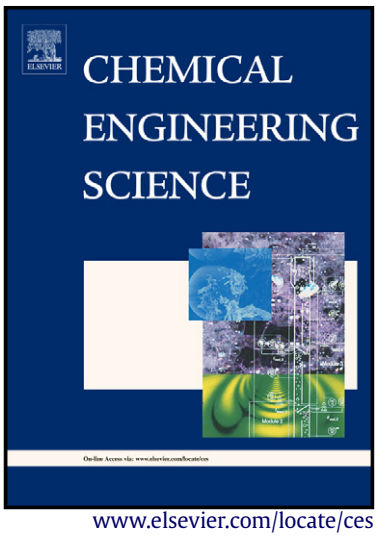

www.elsevier.com/locate/ces

Catalytic performance of cobalt-silica catalyst for Fischer-Tropsch synthesis: Effects of reaction rates on efficiency of liquid synthesis

Nima Moazami, Hamid Mahmoudi, Kiyarash Rahbar, Pooria Panahifar, Athanasios Tsolakis, Miroslaw L Wyszynski

PII: S0009-2509(15)00357-7
DOI: http://dx.doi.org/10.1016/j.ces.2015.05.025
Reference: CES12360

To appear in: *Chemical Engineering Science*

Received date: 24 January 2015
Revised date: 19 April 2015
Accepted date: 15 May 2015

Cite this article as: Nima Moazami, Hamid Mahmoudi, Kiyarash Rahbar, Pooria Panahifar, Athanasios Tsolakis, Miroslaw L Wyszynski, Catalytic performance of cobalt-silica catalyst for Fischer-Tropsch synthesis: Effects of reaction rates on efficiency of liquid synthesis, *Chemical Engineering Science*, http://dx.doi.org/10.1016/j.ces.2015.05.025

Catalytic performance of cobalt-silica catalyst for Fischer-Tropsch synthesis: effects of reaction rates on efficiency of liquid synthesis

Authors: Nima Moazami, Hamid Mahmoudi, Kiyarash Rahbar, Pooria Panahifar, Athanasios Tsolakis, Miroslaw L Wyszynski*

The School of Mechanical Engineering, College of Engineering and Physical Sciences, The University of Birmingham, Edgbaston, Birmingham, B15 2TT, UK
*Corresponding author. Tel: +44 121 414 4159; mobile: +44 7968 157 909
E-mail address: M.L.Wyszynski@bham.ac.uk

Abstract

A one-dimensional pseudo-homogeneous mathematical model of a fixed bed reactor for Fischer-Tropsch (FT) synthesis was developed for the flow of simulated N_2-rich syngas over an in-house cobalt-silica catalyst. This study aims at improving the efficiency of FT synthesis by maximizing the liquid productivities and selectivity, as well as maximizing the syngas conversion and minimizing the methane formation. The developed model predicts the fraction of the reactants and products along the reactor bed length. The rate of syngas conversion and the rate of CO_2, H_2O, CH_4, C_2H_4, C_2H_6, C_3H_8, n-C_4H_{10}, i-C_4H_{10} and $C_{6.05}H_{12.36}$ (C_{5+}) formation were calculated by developing advanced codes in MATLAB. The reaction equations were proposed as a number of lumped chemical reactions (8 reactions, including water gas shift reaction) by means of the molar coefficients of reaction molecules (11 reactive species). The kinetic parameters were estimated by global optimization in MATLAB using the global search method. Optimum values were achieved during the search process. The results predicted by the model were in very good agreement with those measured experimentally at different operating conditions, with respect to conversion and the FT products' selectivity. The rates of production and consumption were derived from a modified power-law rate expression. This study shows that the adapted rate model can deliver a better prediction of final conversion and selectivity. The accuracy of the fitted model relative to the experimental data was determined by a quantitative analysis method using the mean absolute relative residual percentage (MARR %) for the total of 35 data points. It was found that the model based on the modified equation provided a better fit to the experimental data with a MARR of 6.57%, compared to the classic equation with a MARR of 12.24%.

The model predicts the influence of reaction rates on the performance of the fixed bed FT reactor using an unpromoted Co/SiO_2 catalyst at 503 K, 15 bar and 6 L g_{cat}^{-1} h^{-1}. As a result, the conversions of 91.57 and 97.26% were achieved for CO and H_2, respectively with the FT C_{5+} synthesis reaction rate of 7.81×10^{-5} mol g_{cat}^{-1} s^{-1}. The higher rate of C_{5+} formation was found by increasing FT reaction rates compared to the rate of lighter the hydrocarbons' formation. At the same condition, only 5.04 and 8.91% methane and C_2-C_4 selectivity respectively, were predicted; while the highest value of 86.05% liquid (C_{5+}) selectivity was obtained in this case. It was concluded that the higher rate of conversion of H_2 inside the pores filled with liquid products, compared to that of CO, caused an increase in the H_2/CO ratio in the catalyst pores; and thus, a shift towards the formation of lighter hydrocarbons.

Keywords: Fischer-Tropsch synthesis; fixed bed reactor; mathematical modelling; kinetic model

1. Introduction

In biomass to liquid technology where Fischer-Tropsch (FT) synthesis can be the final step there is great potential for the production of ultra-clean transportation fuels like diesel, jet fuel and other hydrocarbon (HC) products [1, 2]. FT synthesis has received considerable worldwide attention, both industrially and academically, due to an increased concern about the problem of environmental pollution and remote gas utilization; as well as the implementation of more stringent environmental legislation on liquid fuels [3, 4]. FT synthesis' products are excellent high-performance, clean diesel fuels; due to the absence of sulphur, their aromatic compounds and their high cetane number. FT synthesis can be defined as the means of indirect coal liquefaction, in which synthesis gas containing CO and H_2 are catalytically converted to a mixture of linear gaseous, liquid and solid hydrocarbons [5]. A wide product spectrum of hydrocarbons is formed by the successive addition of C_1 units (-CH_2- that represents a methylene group) to growing chains on the surface of the catalyst. Equation 1 represents the main reaction of the FT synthesis process [6]. Equation 2 is the methanation reaction which is often considered to be a separate reaction in this process. In addition, Equation 3 is the water gas shift (WGS) reaction. In principle, the WGS reaction is usually considered in the case of an Fe catalyst. With reference to the literature study [7], Co is not very active for the WGS reaction. In contrast, in the present study, the WGS reaction was taken into account since a considerable fraction of water is produced and subsequently CO is converted to CO_2.

$$n\,CO + 2n\,H_2 \rightarrow -(CH_2)_n - + n\,H_2O \qquad \Delta H^{\circ}_{R,298} = -165\ \text{kJ mol}^{-1} \qquad \text{Equation 1}$$

$$CO + 3\,H_2 \rightarrow CH_4 + H_2O \qquad \Delta H^{\circ}_{R,298} = -206\ \text{kJ mol}^{-1} \qquad \text{Equation 2}$$

$$CO + H_2O \leftrightarrow CO_2 + H_2 \qquad \Delta H^{\circ}_{R,298} = -41\ \text{kJ mol}^{-1} \qquad \text{Equation 3}$$

Research studies have shown that only the four group VIII metals, iron (Fe), ruthenium (Ru), cobalt (Co) and nickel (Ni), have sufficiently high activities for FT synthesis. Among them, Fe and Co-based catalysts can be considered as the most practical FT catalysts. The Co-based catalyst has been widely investigated for FT synthesis due to its high selectivity to long chain hydrocarbons (HCs), high FT synthesis activity, high resistance to deactivation by water, low oxygenates selectivity, low water gas shift activity and better catalyst stability in hydrogen-rich environments. In the present work, an in-house developed cobalt catalyst on a silica support (37% Co/SiO_2) was used.

To achieve an optimum in performance for the complete process, the reactor and the kinetic model should be developed mathematically. Also, the details of the products' distribution, selectivity and reactants conversion must be obtained by the model. Generally, various types of reactors including a fixed bed reactor, slurry bed, trickle bed and fluidized bed reactors are used to run the FT synthesis process. The fixed bed reactor has several advantages such as the absence of the requirement to separate the catalyst from the product, the ease of the scaling up from a single tube to a pilot plant, and shutdown robustness compared with slurry bed reactor. However, the downside of fixed bed reactor includes high mass and heat transfer limitation, poor thermal stability, low catalyst reaction rate, offline-slow catalyst replacement, and high capital cost. Shell and Sasol are the pioneers and world leading companies for large scale FT liquids production using fixed bed reactor and slurry bed reactor, respectively. By modelling and optimizing the reactor's operation, it is possible in many cases to achieve significantly enhanced throughput; better and more consistent product quality; rising conversion and selectivity; as well as a significant effect on the scaling up of the processes from the laboratory to production scale. Only a few studies [8-17] are available on the basis of the development of a mathematical model of a fixed bed reactor for FT synthesis.

In addition, the description of the FT kinetics is quite challenging due to the complexity of the reaction pathway and products involved in this process. The kinetics of cobalt-based FT catalysts have been a topic of investigations for decades. The principal governing factors of any FT synthesis kinetic mechanism are the temperature, total pressure, flow rate and the H_2/CO ratio, which affect FT product distribution and conversion rates. There are a number of kinetic studies that were carried out empirically to fit the data based on the power-law rate mechanism. Yang et al. [18] and Wang [19] found empirical rate expressions for supported Co catalysts using a fixed bed reactor via regression of a power-law equation. Zennaro et al. [20] studied the kinetics on a

well-characterized 11.7% Co/TiO_2 catalyst in a differential fixed bed reactor. The experimental data of this study were fitted by a power-law expression. Das et al. [21] investigated the kinetics and effects of water for a 12.4 wt % Co/SiO_2 catalyst using a 1-L continuously stirred tank reactor (CSTR). The measured data of this study were also fitted by a power-law expression. Marvast et al. [22] modelled a two-dimensional fixed bed FT reactor packed with an Fe-HZSM5 catalyst using the same approach. According to this study, the C_{5+} fraction was lumped in a single kinetic equation as representative FT products. However, their results (for rate of conversion and production) were not sufficiently accurate, with a relatively large error carried by the model. Jarosch et al. [23] developed a model using a similar approach for a Co:Re (21:1) catalyst on γ-Al_2O_3. Another relevant example is the work done by Ma et al. [24, 25] that was applied to a 25% Co/Al_2O_3 catalyst to fit the CH_4 kinetic data. Overall, the kinetic study based on the power-law rate model can be a powerful method to provide some insight into FT synthesis, without the need to represent a complex reaction network.

No-one has yet published the mathematical model of a fixed bed reactor over a Co/SiO_2 FT catalyst, including the reaction kinetics with the details of production rates of CO_2, H_2O, CH_4, C_2, C_3, C_4 and C_{5+} as well as the CO and H_2 conversion for this case. In the present study, a simple one-dimensional pseudo-homogeneous mathematical model of a fixed bed reactor is developed. The reaction kinetics were proposed on a 37% Co/SiO_2 catalyst using the modified power-law rate expression. The model predicts a mole fraction of the proposed species at five different sets of experimental conditions in which the data sets were adequate for this study. A parametric sensitivity analysis, with a detailed numerical simulation, is performed to illustrate the effects of reaction rates on the efficiency and performance of FT synthesis with respect to productivity, selectivity and conversion.

2. Experimental set-up

Figure 1 indicates the schematic diagram of the experimental setup (designed by co-worker [26]) that was conducted in a fixed bed reactor packed with 37 wt% Co catalysts on a silica support. The experiments were carried out at five different operating conditions with respect to the temperature, pressure and flow rate; they are tabulated in Table 1. The details of the reactor, as well as the in-house spherical Co catalyst and commercial silica support's (provided by Fuji Silysia Chemical Ltd) specification, are tabulated in Table 2. A mini-structured vertical downdraft fixed bed reactor was used for the FT synthesis. The reactor was fixed in a tube furnace in order to provide the heat zone and a cast iron jacket was installed between the furnace and reactor to provide the uniform wall temperature. A simulated N_2-rich syngas bottle of 17% CO, 33% H_2 and 50% N_2 was fed into the reactor column at each experiment. Silicon carbide was used to dilute 2 g of the catalyst with a mass ratio of 1:12 (Co-SiO_2/SiC) for each experiment and then it was loaded into the reactor. A calibrated smart mass flow controller was employed to regulate the flow rate of the syngas (Bronkhorst Ltd).

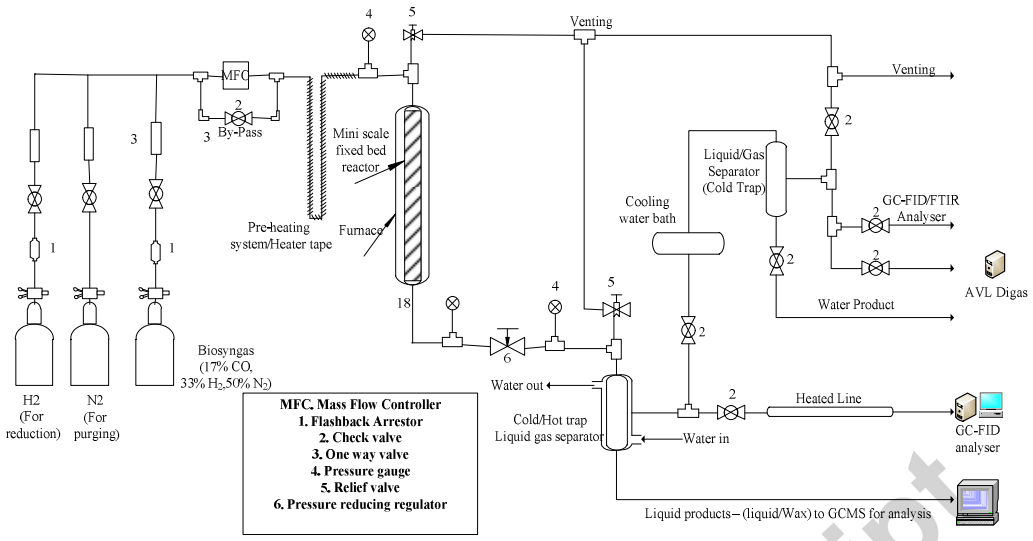

Figure 1 Schematic diagram of the experimental setup [27].

Nitrogen gas was used to purge the reactor bed. Prior to the reaction, the catalyst was reduced in order to be activated. The catalyst was placed on stream for a 12 h reaction time to measure CO conversion, selectivity and productivity of hydrocarbon synthesis, as well as CH_4 and CO_2 product species. Two liquid/gas separators were used to separate liquid products from the gaseous stream. Changes in the concentration of CO and CO_2 production were monitored online by using a modified CO analyser (AVL Digas 440). A Gas Chromatogram Flame Ionization detector (GC-FID) (HP 5890) was employed to analyse the HC_1-HC_8 online. The heavier liquid products were analysed offline by using Gas Chromatogram-Mass Spectrometry (GC-MS) (PerkinElmer ^{TM}). Utilization of nitrogen-rich syngas (with 50% of N_2 (volumetric percentage)) leads to reduction in production cost of diesel oil by eliminating the need for application of gas recycling loop after production of syngas by air partial oxidation. Waste generated heat of FT reaction could be removed effectively and temperature runaway probability can be minimized by nitrogen gas. Utilization of nitrogen as an inert in FT regime could result in an increase in tube diameter of reactor and decrease in number of tubes without temperature runaway problem [11].

Table 1 Experimental conditions of the present study

Experiment	Temperature [K]	Pressure [bar]	WHSV [L g_{cat}^{-1} h^{-1}]
Condition 1	503	15	2.4
Condition 2	503	20	3.0
Condition 3	503	25	3.6
Condition 4	518	10	2.4
Condition 5	528	10	3.0

Table 2 The details of the fixed bed reactor and catalyst/support used in the present study [27]

Parameter	Unit	Value
Reactor length	cm	52.83
Reactor bed length	cm	11
Outer tube diameter	mm	19.05
Inner tube diameter	mm	15.7
Tube wall thickness	mm	1.65
Active site volume fraction	(-)	0.25
Void fraction	(-)	0.4

Bulk density of support catalyst	g ml^{-1}	0.38
Particle diameter	µm	150
Catalyst/support weight	g	2.0
Surface area	m^2 g^{-1}	257
Water content	wt %	0.6
Pore volume	ml g^{-1}	1.20
No. of species	-	12
No. of reactions	-	8

3. Development of the reactor mathematical model

3.1. Mathematical reactor model and kinetic description

A numerical one-dimensional mathematical model was developed to represent the process of FT synthesis using the mini-scale fixed bed reactor. The model was assumed to proceed isothermally for the proposed range of operating conditions. To develop the mass balance equation, a differential equation was used to determine the gradient of the change of concentration and partial pressure of the components against the axial dimension of the reactor bed length. Equations 4 and 5 describe the mole balance of the species '*i*' with respect to concentration and partial pressure, respectively. The mole balance equations were first order ordinary differential equations (ODEs). The effects of axial dispersion, interphase and intraparticle mass transport were not taken into account. A series of eggshell cobalt catalyst supported with silica powder with dissimilar structure were used. The utilization of eggshell catalyst in mini scale bio-diesel generator is an innovative intension which could overcome the mass transfer limitation in fixed-bed reactor system [26]. Eggshell catalysts have been proposed to overcome difficulties due to diffusion limitations in catalyst pellets in fixed bed reactors and this application (of eggshell catalysts) was also reported by literature [28]. Also, the catalyst was loaded in the reactor in powder form (2 g catalyst with particle size of 75-150 µm) in order to prevent internal mass transfer limitations. Similar to this, Visconti et al. [29] studied the detailed kinetics of the Fischer-Tropsch synthesis on cobalt catalyst in the form of powder to prevent the internal mass transfer limitations. The mixture velocity was calculated from the continuity equation (Equation 6). The density of the fluid was computed by applying the chain rule to the ideal gas law (Equation 7). The classic Ergun law for laminar flow was applied to calculate the overall pressure drop (Equation 8). Several parameterizations for the friction factor, 'f', have been given in the literature [30]. Equation 9 was used, which is valid for laminar flow for spheres over a relatively broad range of particle Reynolds numbers. Equation 10 is the size of the mesh in which the model was discretized in the dimension needed by the code (i.e. ''z'', ''i''and ''t'' which are length, species and number of experimental conditions, respectively) [31]. Table 3 lists the important equations and correlations that were employed in the present model [27].

$$u_s \frac{dC_i}{dz} = \rho_B \beta \sum_{j=1}^{NR} v_{ij} R_j - C_i \frac{du_s}{dz} \quad \text{Equation 4}$$

$$\frac{u_s}{R_g T} \frac{dp_i}{dz} = \rho_B \beta \sum_{j=1}^{NR} v_{ij} R_j - \left(\frac{p_T}{R_g T} \frac{du_s}{dz} \right) \quad \text{Equation 5}$$

$$\rho_f \frac{du_s}{dz} = -u_s \frac{d\rho_f}{dz} \quad \text{Equation 6}$$

$$\frac{d\rho_f}{dz} = \frac{d\left(\frac{p_T M_m}{R_g T}\right)}{dz} \frac{M_m}{R_g} \left[\frac{1}{T} \frac{dp_T}{dz} \right] \quad \text{Equation 7}$$

$$\frac{dp_T}{dz} = -f \frac{u_s^2 \rho_f}{d_p} \quad \text{Equation 8}$$

$$f = \frac{(1-\varepsilon)^2}{\varepsilon^3} \frac{36(25/6)}{Re} \quad \text{Equation 9}$$

$$Size\ of\ the\ mesh = [Number\ of\ nodes\ in\ z\ direction] \times [Number\ of\ species] \times [Number\ of\ expeirntal\ conditions]$$ Equation 10

Table 3 Correlations and equations used in this study

Parameter	Equation		Reference
Species concentration	$C_i = \frac{Y_i p_T}{R_g T}$	Equation 11	[32]
Reynolds number	$Re = \frac{\rho_f u_s d_p}{\mu_m}$	Equation 12	[33]
Mixture viscosity	$\mu_m = \sum_{i=1}^{NS} Y_i \mu_i$	Equation 13	[34]
Mixture molecular weight	$M_m = \sum_{i=1}^{NS} Y_i M_i$	Equation 14	[34]
Species viscosity	$\mu_i = a + bT + cT^2 + dT^3$	Equation 15	[35]
Initial fluid density	$\rho_f = \frac{p_T M_m}{R_g T}$	Equation 16	
Initial superficial velocity	$u_{s,0} = \frac{Q}{A_r}$	Equation 17	
Conversion of reactants	$x_i = \frac{C_{i,in} - C_{i,out}}{C_{i,in}} \times 100$	Equation 18	
CO_2 selectivity	$S_{CO2} = \frac{C_{CO2,out}}{C_{CO,in} - C_{CO,out}} \times 100$	Equation 19	[36]
Light hydrocarbons selectivity	$S_{C_i} = \frac{C_{i,out}}{C_{CO,in} - C_{CO,out} - C_{CO_2,out}} \times 100\ for\ 1 \le i \le 4$	Equation 20	
Total liquid hydrocarbon selectivity	$S_{C_{5+}} = 100 - (S_{C_1} + S_{C_2} + S_{C_3} + S_{C_4})$	Equation 21	

In order to complete the mathematical description of the reactor model, the details relating to the kinetics of the reactions, need to be provided. Kinetic models of reduced complexity are attractive for reactor analysis and design purposes. The FT synthesis kinetic mechanism is based on a complex reaction system with many chemical compounds. The reaction network can be classified as a number of lumped reactions by means of the kinetic characteristics of reaction molecules. These models are capable of capturing the essential features of the FT synthesis products' distribution without the need for a parameter, such as chain growth probability (α).

In the present work, the rate of CO and H_2 disappearance and the rate of CO_2, H_2O, CH_4, C_2H_4, C_2H_6, C_3H_8, n-C_4H_{10}, i-C_4H_{10} and $C_{6.05}H_{12.36}$ (C_{5+}) formation were taken into account. The reaction equations were proposed as a number of lumped reactions (Equations 22-29) by means of the kinetic characteristics of reaction molecules for FT synthesis over Co/SiO_2 (Table 4). Equation 29 is the representative single reaction equation that corresponds the lumped rate of C_{5+} formation by setting $C_{6.05}H_{12.36}$ as the average molecular value of liquid HC components.

Table 4 Postulated lumped FT synthesis kinetic model over Co/SiO_2 and estimated kinetic parameters

Assumed reaction pathway		n_j	m_j	δ_j	α_j	E_j
$CO + 3H_2 \xrightarrow{R_1} CH_4 + H_2O$	Equation 22	0.38	0.15	1.99	65.56	99.79
$2CO + 4H_2 \xrightarrow{R_2} C_2H_4 + 2H_2O$	Equation 23	-1.17	1.80	-2.05	4.54×10^{-2}	72.51
$2CO + 5H_2 \xrightarrow{R_3} C_2H_6 + 2H_2O$	Equation 24	0.81	-2.00	1.73	1.14×10^{-3}	48.51

$3CO + 7H_2 \xrightarrow{R_4} C_3H_8 + 3H_2O$	Equation 25	-1.03	1.70	-0.41	1.19×10^{-6}	31.03
$4CO + 9H_2 \xrightarrow{R_5} n\text{-}C_4H_{10} + 4H_2O$	Equation 26	-0.86	1.38	0.68	1.84×10^{-10}	27.59
$4CO + 9H_2 \xrightarrow{R_6} i\text{-}C_4H_{10} + 4H_2O$	Equation 27	-0.69	1.25	2.21	6.59×10^{-9}	10.14
$6.05CO + 12.23H_2 \xrightarrow{R_7} C_{6.05}H_{12.36}\ (C_{5+}) + 6.05H_2O$	Equation 28	1.71	-1.00	-2.57	1.98×10^{-8}	12.44
$CO + H_2O \xrightarrow{R_8} CO_2 + H_2$	Equation 29	-1.71	1.57	2.98	3.78×10^{-5}	10.00

The kinetic parameters in Table 4 were estimated by global optimization in MATLAB using a global search method. This method was applied as an alternative to the traditional (gradient-based) optimization methods to avoid convergence to the local minima during the search process. Optimum values were achieved during the search process and they were not significantly different. These values were also determined within the acceptable range compared to the literature values. The modified power-law rate expression (Equation 30) was derived to calculate the rate of consumption and production of the species mentioned above.

$$r_j = \alpha_j(\frac{T}{T_r})^{\delta_j}\exp\left(-\frac{E_j}{R_g T}\right)p_{CO}^{n_j}p_{H2}^{m_j} \qquad \text{Equation 30}$$

In this equation, p_{CO} and p_{H_2} stand for partial pressure of CO and H_2, respectively; α_j and δ_j stand for the pre-exponential factor and the explicit temperature dependence factor of the pre-exponential factor of rate constant, respectively. In this equation, E_j denotes the activation energy of the j^{th} reaction equation; n_j and m_j indicate the order of reaction with respect to CO and H_2, respectively.

4. Results and discussion

4.1. Model prediction

Optimal values of kinetic parameters were calculated by minimizing a multi-criteria objective function, Equation 31. This function is based on the sum of the absolute relative deviation percentage of seven species at five proposed experimental conditions.

$$F_{obj} = \sum_{j=1}^{n_{exp}}\sum_{i=1}^{n_{sp}} w_{i,j}\left(\left|\frac{y_{i,j}^{exp} - y_{i,j}^{cal}}{y_{i,j}^{exp}}\right| \times 100\right) \qquad \text{Equation 31}$$

In this equation, n_{sp} denotes the total number of species (CO, CO_2, CH_4, C_2, C_3, C_4 and C_{5+}) and n_{exp} shows the total number of experimental conditions; $y_{i,j}^{exp}$ and $y_{i,j}^{cal}$ terms are the experimental and calculated values, respectively and take reactants conversion and products selectivity into account, for the i^{th} component and j^{th} experiment; and w_i corresponds to the different weights taken to normalize the contributions of each species.

A qualitative analysis of the predicted results by the model was illustrated in Figure 2. The model's results were compared against measured data using a parity diagram. The majority of the data points were between -10% and +10% error. This comparison was carried out with respect to the selectivity of CO_2, CH_4, C_2, C_3, C_4 and C_{5+} as well as CO conversion at five different experimental conditions. Therefore, a total number of 35 data points were investigated, which were enough for the present analysis.

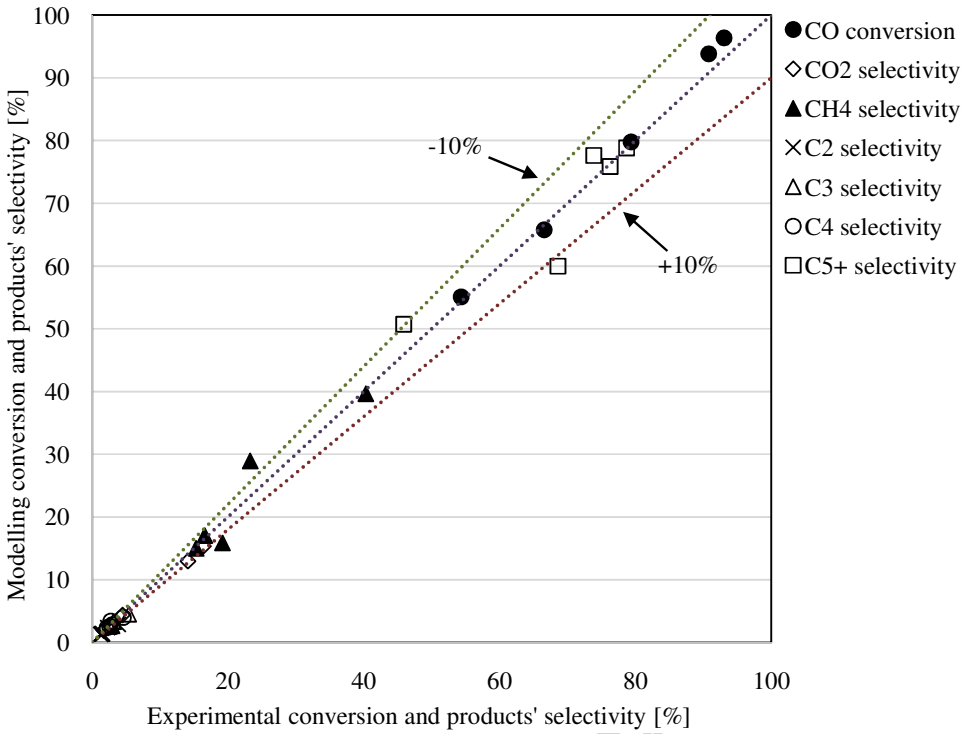

Figure 2 The parity of the calculated CO_2, CH_4, C_2, C_3, C_4 and C_{5+} selectivity as well as CO conversion against experimental results, using the modified power-law rate expression, with the total of 35 data points.

Table 5 shows the results obtained by the model (the modified power-law rate model) and those measured by experiments with respect to CO conversion and products' selectivity. The modelling results were in good agreement with the experimental data. The accuracy of the fitted model relative to the experimental data was determined by a quantitative analysis method using the mean absolute relative residual percentage (MARR %). It was found that the model based on the modified equation provided a better fit to the experimental data with a MARR of 6.57% compared to the classic equation with MARR of 12.24%.

$$MARR(\%) = \frac{1}{n_{exp} n_{sp}} \sum_{j=1}^{N_{exp}} \left[\sum_{i=1}^{N_{sp}} \left(\left| \frac{y_{i,j}^{exp} - y_{i,j}^{cal}}{y_{i,j}^{exp}} \right| \times 100 \right) \right] \quad \text{Equation 32}$$

Table 5 A comparison of the results obtained by the model (Mod.) with experimental data (Exp.) with respect to CO_2, CH_4, C_2, C_3, C_4 and C_{5+} selectivity as well as CO conversion at operating conditions 1 to 5

	Condition 1		Condition 2		Condition 3		Condition 4		Condition 5	
Component (%)	Exp.	Mod.	Exp.	Mod.	Exp.	Mod.	Exp.	Mod.	Exp.	Mod.
CO Conversion	79.34	79.76	66.55	65.80	54.34	55.11	93.03	96.35	90.78	93.83
CO_2 Selectivity	4.46	4.38	2.63	2.66	1.72	1.92	14.10	12.98	16.38	15.37
CH_4 Selectivity	16.58	17.03	19.20	15.85	15.32	15.01	23.27	28.94	40.29	39.67
C_2 Selectivity	1.47	1.47	1.52	1.35	1.27	1.28	2.28	2.36	3.86	2.90
C_3 Selectivity	2.79	2.80	2.90	2.63	2.51	2.53	3.14	3.29	5.37	4.50
C_4 Selectivity	2.93	2.85	2.53	2.55	2.18	2.36	2.74	3.43	4.60	4.00
C_{5+} Selectivity	76.24	75.85	73.85	77.62	78.71	78.81	68.57	61.98	45.88	48.93

A good agreement was achieved based on the CO_2 production rate in all the experimental data set. This confirms the validity of the model and reaction equations to predict the rate of CO_2 formation. Similarly, CO conversion was predicted very well except in a higher temperature condition (condition 5). The main difference was achieved with respect to the CH_4 formation, rate especially at conditions 2 and 4. Overall, the predicted values were in good agreement with the experimental data.

According to the results, 90.78% CO conversion was achieved at condition 5. At the same condition, the undesirable CH_4 selectivity was 40.29%, which is very high compared to other operating conditions. Also, the results indicate that the methane rate of formation was remarkably higher compared to higher paraffinic hydrocarbons. This can be due to the lower energy barrier of methane for formation, compared to other paraffins [37, 38]; however, in contrast the E_{CH4} value was higher. Mathematically, the higher the value of the activation energy, the lower the value of the exponential term in the reaction equation. Regardless of the value of the pre-exponential factor, it can be concluded that the higher value of formation rate corresponds to the lower value of the energy barrier. This contradiction was explained by the fact that the pre-exponential value of methane was far greater than other paraffins that result in a higher methane formation rate and subsequently higher selectivity value, compared to C_2-C_4. In Figure 3, the axial conversion profiles of CO and H_2 species are depicted along the reactor bed length. As it can be seen, the gradients of the conversion's profile of the syngas components are slowed down in all experimental data sets as they proceeded to the reactor outlet. The decreasing of CO and H_2 mole fractions results in a reduction in concentration of syngas components and an increase in the conversion.

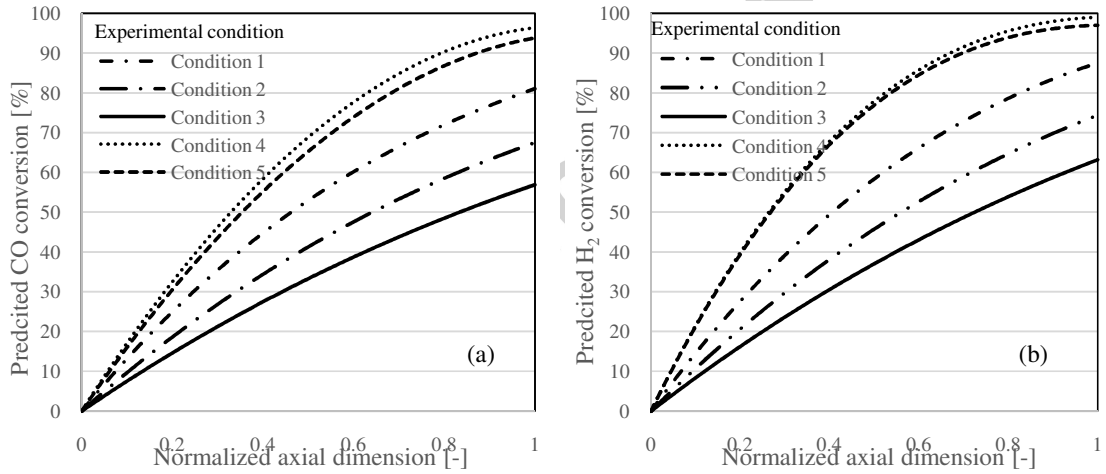

Figure 3 FT-conversion profiles predicted by the mathematical model with respect to (a) CO and (b) H_2 at five different operating conditions shown in Table 1.

4.2. Effects of FT reaction rate

Literature studies showed [39, 40] that the promoted Co-based catalyst had higher CO hydrogenation rates than an unprompted Co catalyst. The catalyst activity strongly depended on its weight fraction and the addition of a promoter in the solid catalyst. The addition of a promoter to a Co-based catalyst tripled the activity of the catalyst and increased the C_{5+} selectivity from 84% to 91% [39]. The results revealed by the present study, indicate that the cobalt particle size was controlled by utilizing mesoporous support SiO_2 to achieve the highly reducible and dispersed active phase; as well as preventing the sintering of particles. Although the Co catalyst used in this study was an unprompted catalyst, it was very active due to the high percentage of cobalt content (37%). A higher amount of Co catalyst in the reactor bed is associated with its activity, which causes an increase in the rates of the FT reaction and therefore the CO and H_2 conversion.

The effects of the FT reaction rates on CO and H_2 conversion as well as selectivity of CO_2, CH_4 C_2, C_3, C_4, and C_{5+} were investigated at 503 K, 15 bar and 6 L g_{cat}^{-1} h^{-1}. In order to minimize the effect of the highly exothermic methanation reaction, the high value of the flow rate was taken into account. Figure 5 shows CO and

H_2 conversion as well as CO_2, CH_4, C_2, C_3, C_4, and C_{5+} selectivity as the function of the FT reaction rates. Light HC products (i.e. C_2-C_4) increased slowly with an increase in FT reaction rates. The results showed that the rate of conversion of CO and H_2 strongly depended on the FT reaction rates, increasing along with their increases. It was found that the rate of conversion of H_2 is slightly greater than CO (Figure 4). By increasing the FT reaction rates from 1.95×10^{-5} to 7.81×10^{-5} mol g_{cat}^{-1} s^{-1} the conversion of CO and H_2 increased by 46.76% and 47.79%, respectively (Table 6). Figure 5 shows higher methane selectivity was predicted at smaller FT reaction rates. Methane selectivity drops from 15.86 to 5.04% as the FT reaction rates increase from 1.95×10^{-5} to 7.81×10^{-5} mol g_{cat}^{-1} s^{-1}. Based on literature studies, FT reaction rates increase as pore size increases. Higher reducibility of large cobalt particles is likely to be one of the reasons for the higher FT reaction rates and lower methane selectivity on wider pore cobalt catalysts. The higher rate of C_{5+} formation was found with increasing the FT reaction rates (from R_{FT} (1) to (6)), compared to the rate of lighter HCs formation. It was suggested that this can be due to a greater rate of conversion of H_2 (R_{FT} (6)) inside pores filled with liquid products, compared to that of CO, caused an increase in the H_2/CO ratio in the catalyst's pores; and thus there is a shift towards the formation of lighter HCs. The FT reaction rates increase with an increase in pore size. The catalyst with a small pore diameter exhibits low activity; a significant increase in FT reaction rates can be observed by increasing the pore size. The higher methane formation rate and lower C_{5+} selectivity can be expected with a small pore size. Catalyst characterization carried out by Khodakov et al. [28] revealed that a thin pore catalyst contained smaller cobalt particles. Thus, the activity of the catalysts seems to be affected by the size of the cobalt particles. The FT reaction rates were found to be lower for smaller particles than for larger particles. The lower FT reaction rates, the higher the selectivity of CH_4 and the lower the C_{5+} selectivity.

The trend of changes of CO_2 selectivity was found to be slightly different from other observations. Table 6 shows the CO_2 selectivity was reduced first with the increasing of the FT reaction rates at lower rates (from 1.95×10^{-5} to 4.88×10^{-5} mol g_{cat}^{-1} s^{-1}) and then its value was increased with the further raising of FT reaction rates; probably because CO_2 was produced via water gas shift reaction from the reaction between CO and water. An increase of FT reaction rates increased the rate of CO conversion, which is related to a decrease of CO mole fraction. The water was produced as the reaction occurred at the surface of the catalyst. It was attributed to the observed increase in the rate of growing of the H_2O fraction with the increasing of the FT reaction rates; however, the rate of CO mole fraction reduction (i.e. the slope of CO consumption rate) reduces by the increasing of the FT reaction rates. At some point, the rate of the H_2O formation is more than the rate of reduction of the CO mole fraction and therefore could result in increasing CO_2 selectivity.

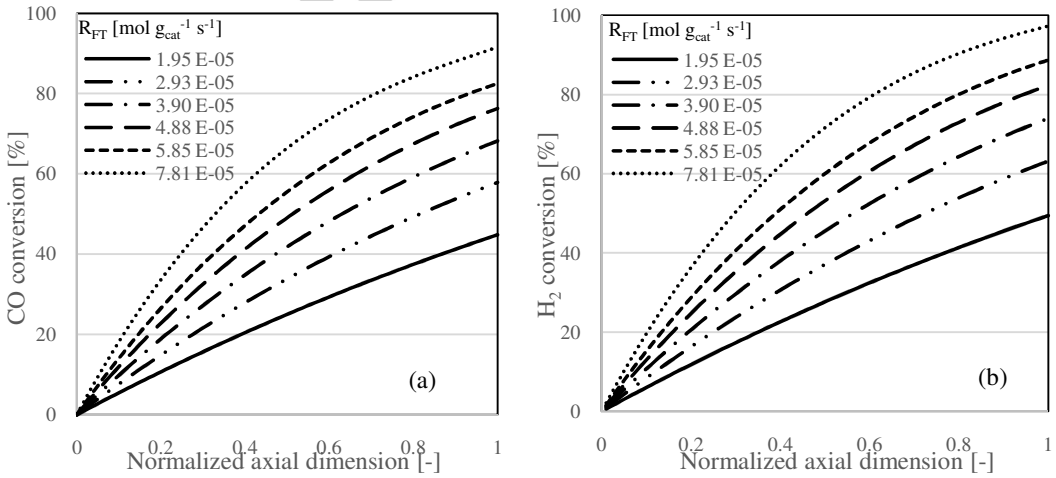

Figure 4 The conversion profiles of (a) CO and (b) H_2 species along the reactor bed length (normalized axial dimension) at different FT reaction rate values. The results are based on the developed mathematical model.

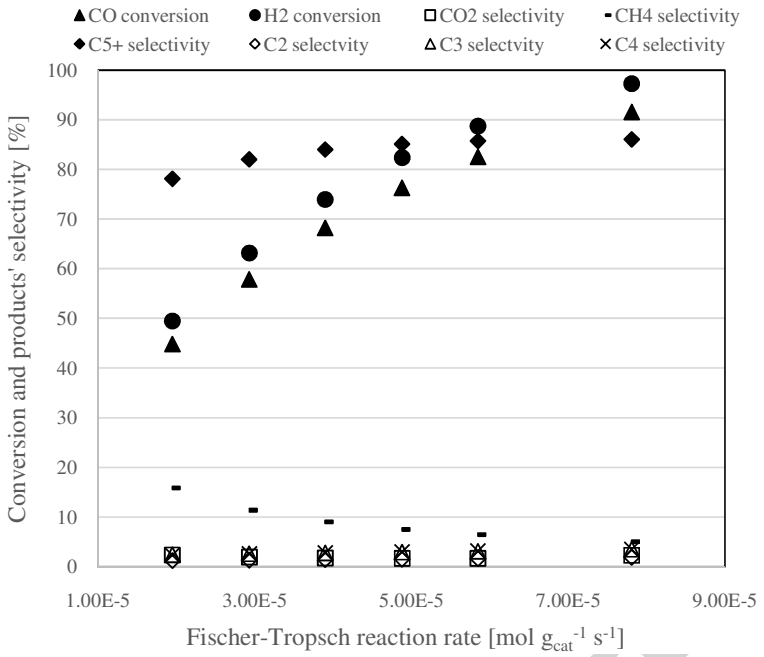

Figure 5 The Effects of FT reaction rate on CO and H_2 conversion as well as selectivity of CO_2, CH_4 C_2, C_3, C_4, and C_{5+}. Reaction conditions: 503 K, 15 bar and 6 L g_{cat}^{-1} h^{-1}.

Table 6 The values of final syngas conversion and products' selectivity obtained by the model at different FT reaction rate values

Components (%)	R_{FT} (1) 1.95E-05	R_{FT} (2) 2.93E-05	R_{FT} (3) 3.9E-05	R_{FT} (4) 4.88E-05	R_{FT} (5) 5.85E-05	R_{FT} (6) 7.81E-05
CO conversion	44.81	57.86	68.22	76.29	82.52	91.57
H_2 conversion	49.47	63.15	73.97	82.35	88.72	97.26
CO_2 selectivity	2.40	1.95	1.75	1.69	1.73	2.33
CH_4 selectivity	15.86	11.42	9.01	7.50	6.45	5.04
C_2 selectivity	1.23	1.34	1.43	1.52	1.62	1.88
C_3 selectivity	2.40	2.60	2.76	2.92	3.08	3.50
C_4 selectivity	2.38	2.60	2.78	2.95	3.13	3.53
C_{5+} selectivity	78.13	82.04	84.02	85.11	85.72	86.05

4.3. Effect of water gas shift reaction rate

In principle, WGS reaction is usually considered in the case of Fe catalysts. With reference to a literature study [7], Co is not very active for WGS reaction. It means that the effects of water were normally not considered in the kinetics of FT synthesis with cobalt catalysts. Some studies showed that the WGS reaction occurred to a small extent, acting as a one-way reaction and producing a small amount of carbon dioxide. In this case, carbon dioxide is typically treated as a carbon-containing product. In the present model, the CO_2 formation was non-negligible and H_2O partial pressure was identified as one of the key factors influencing the reaction rate; this leads to the conclusion that the WGS reaction is responsible for this result. As explained above, this reaction is a very well-known reversible process; however, the best fit of the experimental data corresponded to a model postulating the irreversibility of CO_2 formation.

The amount of catalyst active sites available for the FT reaction changes with the partial pressures of water and hydrogen. The presence of hydrogen prevents the catalyst from oxidation when the water's partial pressure

is not too high to cause permanent deactivation. In contrast, water functions by reoxidizing the cobalt catalysts which turns into an activity loss for the FT reaction [41].

The effects of WGS reaction rate on conversion, rate of formation and selectivity were studied at a temperature of 503 K, a total pressure of 15 bar and a flow rate of 6 L g_{cat}^{-1} h^{-1}. Figure 6 illustrates the trend of the changes in CO and H_2 conversion at different WGS reaction rates along the normalized axial dimension (reactor bed length). Figure 7 shows that the effects of WGS reaction rate on HCs' selectivity and rate of each formation was almost negligible. The conversion rate of CO was slightly changed with WGS reaction rates, increasing with increases in the WGS reaction rate. In contrast, the increases in the WGS reaction rates did not change the H_2 conversion rate (Figure 6). The WGS reaction rates were found to be effective on the rate of unwanted CO_2 formation, increasing from 2.40 to 8.37% with increases in WGS reaction rates from 1.04×10^{-6} to 4.16×10^{-6} mol g_{cat}^{-1} s^{-1} (Table 7).

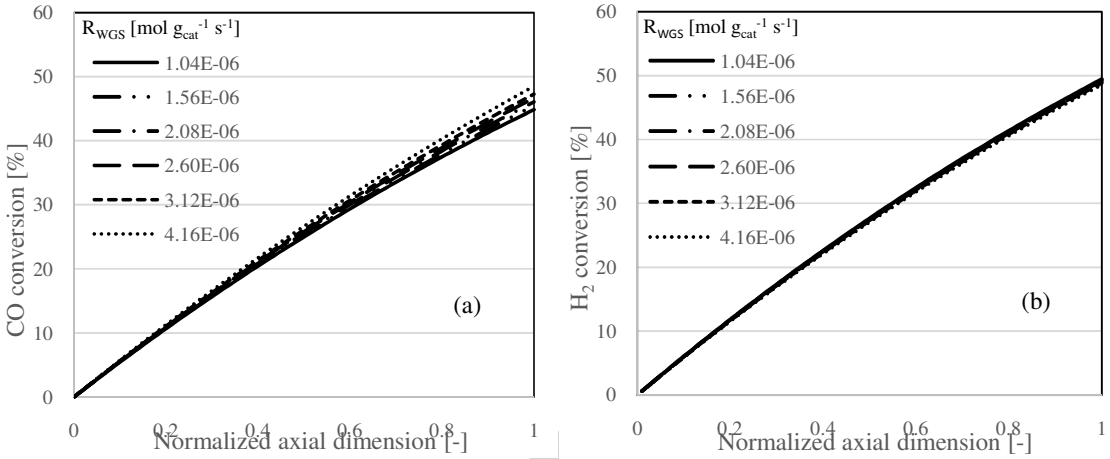

Figure 6 (a) CO and (b) H_2 conversion profiles along the reactor bed length (normalized axial dimension) at different water gas shift reaction rate values. The results are based on the developed mathematical model.

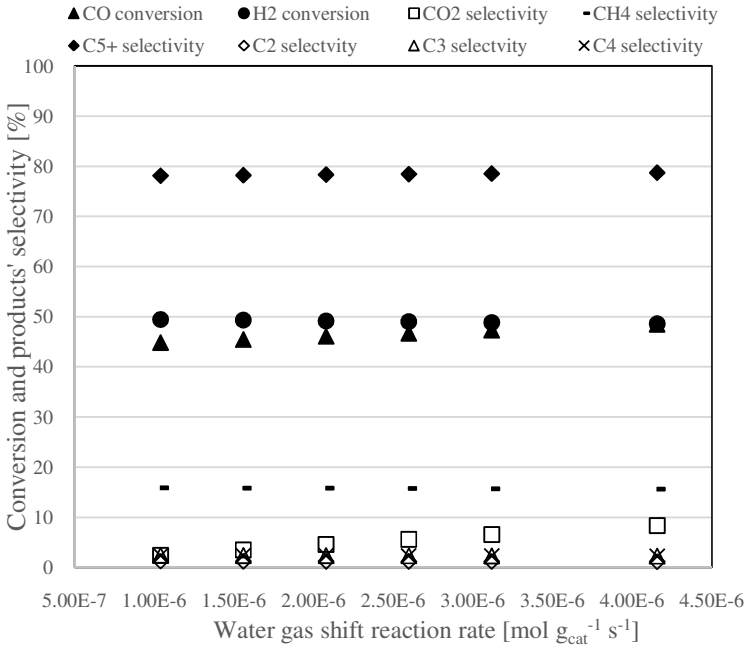

Figure 7 Effects of WGS reaction rate on CO and H_2 conversion as well as selectivity of CO_2, CH_4 C_2, C_3, C_4, and C_{5+}. Reaction conditions: 503 K, 15 bar and 6 L g_{cat}^{-1} h^{-1}.

Table 7 The values of final syngas conversion and products' selectivity obtained by the model at different water gas shift reaction rate values.

Components (%)	R_{WGS} (1) 1.04E-06	R_{WGS} (2) 1.56E-06	R_{WGS} (3) 2.08E-06	R_{WGS} (4) 2.60E-06	R_{WGS} (5) 3.12E-06	R_{WGS} (6) 4.16E-06
CO conversion	44.81	45.44	46.06	46.68	47.28	48.47
H_2 conversion	49.47	49.31	49.15	49.01	48.86	48.59
CO_2 selectivity	2.40	3.51	4.57	5.59	6.56	8.37
CH_4 selectivity	15.86	15.82	15.77	15.73	15.69	15.60
C_2 selectivity	1.23	1.22	1.20	1.19	1.17	1.15
C_3 selectivity	2.40	2.37	2.35	2.32	2.30	2.25
C_4 selectivity	2.38	2.36	2.34	2.32	2.30	2.26
C_{5+} selectivity	78.13	78.23	78.34	78.44	78.53	78.73

4.4. Effect of methane formation reaction rate

Methane formation via methanation reaction is one of the primary variables affecting any FT synthesis process. Methane formation controls the most valuable FT products' selectivity, which are liquid HCs in this case [42]. The results showed that a higher CH_4 selectivity of the Co catalyst is primarily correspondent to a higher CH_4 rate constant, compared with other lighter HCs' formation (C_2-C_4). This conclusion is consistent with the previous report from the literature [25].

Figure 8 illustrates the trend of changes in CO and H_2 conversion at different methanation reaction rates along the normalized axial dimension. The rate of conversion of CO and H_2 strongly depend on the methanation reaction rate, increasing with increases in the rate values. It was found that the rate of conversion of H_2 is greater than CO (Figure 8). By increasing the methanation reaction rate from 4.40×10^{-6} to 1.76×10^{-5} mol g_{cat}^{-1} s^{-1} the conversion of CO and H_2 increased by 12.62% and 21.85%, respectively (Table 8). Figure 9 shows CO and H_2 conversion as well as CO_2, CH_4, C_2, C_3, C_4, and C_{5+} selectivity as functions of the methanation reaction rate. The effects of the methanation reaction rate on CO_2 formation and lighter HCs' selectivity, excluding CH_4, were almost negligible. The results showed that the rate of CH_4 formation and C_{5+} strongly depend on the methanation reaction rate. It was apparently found by increasing the methanation reaction rate that the selectivity of CH_4 increased, while liquid formation dropped significantly. By increasing the methanation reaction rate from 4.40×10^{-6} to 1.76×10^{-5} mol g_{cat}^{-1} s^{-1} the CH_4 selectivity increased by 28.82% and the C_{5+} selectivity decreased by 27.63%, (Table 8).

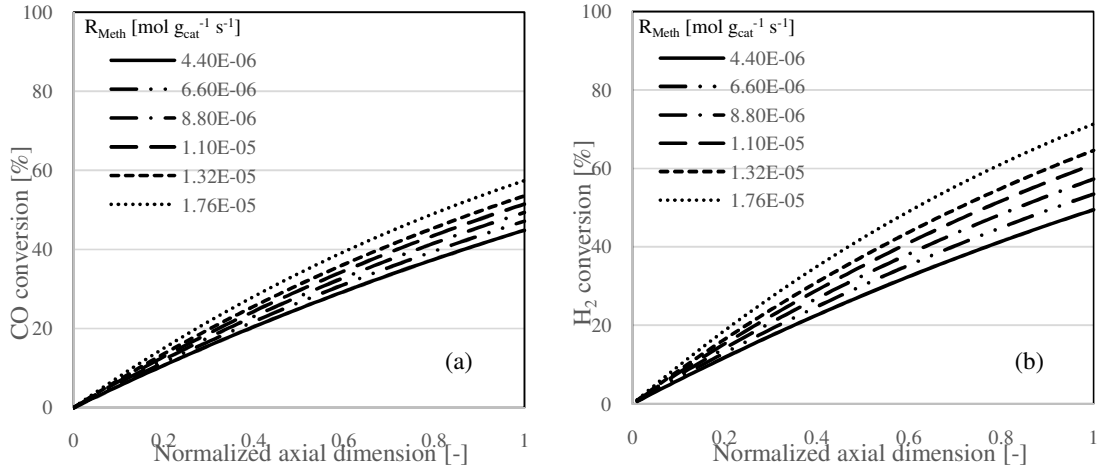

Figure 8 The conversion profiles of (a) CO and (b) H_2 species along the reactor bed length (normalized axial dimension) at different methanation reaction rate values. The results are based on the developed mathematical model.

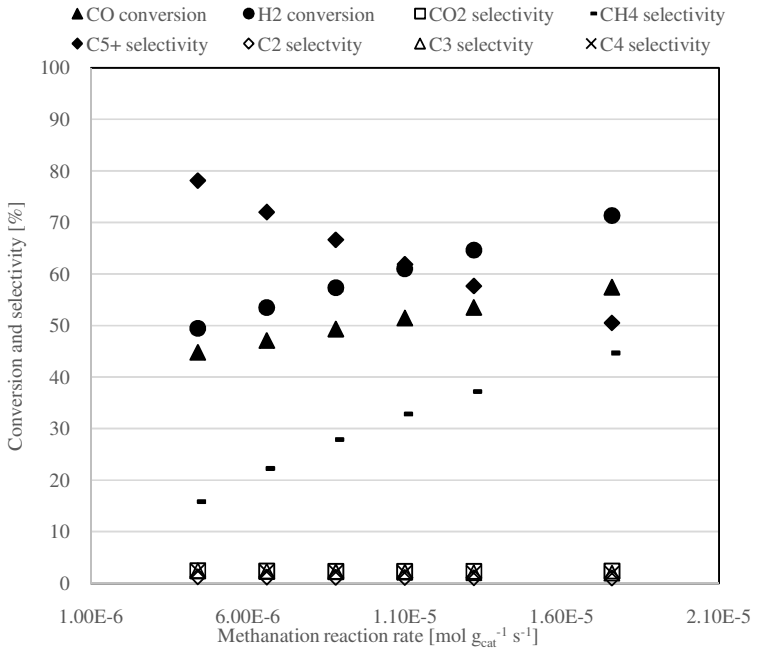

Figure 9 Effects of methanation reaction rate on CO and H_2 conversion as well as selectivity of CO_2, CH_4 C_2, C_3, C_4, and C_{5+}. Reaction conditions: 503 K, 15 bar and 6 L g_{cat}^{-1} h^{-1}.

Table 8 The values of final syngas conversion and products' selectivity obtained by the model at different methanation reaction rate values

	R_{Meth} (1)	R_{Meth} (2)	R_{Meth} (3)	R_{Meth} (4)	R_{Meth} (5)	R_{Meth} (6)
Components (%)	4.40E-06	6.60E-06	8.80E-06	1.10E-05	1.32E-05	1.76E-05
CO conversion	44.81	47.11	49.32	51.46	53.52	57.43
H_2 conversion	49.47	53.47	57.33	61.04	64.61	71.32
CO_2 selectivity	2.40	2.35	2.33	2.32	2.32	2.37
CH_4 selectivity	15.86	22.25	27.87	32.83	37.23	44.69
C_2 selectivity	1.23	1.17	1.13	1.09	1.06	1.01
C_3 selectivity	2.40	2.29	2.19	2.11	2.04	1.93
C_4 selectivity	2.38	2.26	2.16	2.07	2.00	1.87
C_{5+} selectivity	78.13	72.02	66.65	61.90	57.67	50.50

5. Conclusion

A mathematical model of a fixed bed reactor for Fischer-Tropsch (FT) synthesis was developed by a one-dimensional pseudo-homogeneous flow over simulated N_2-rich syngas on an in-house Co/SiO_2 catalyst. The reaction equations were proposed as a number of lumped reactions by means of the molar coefficient of the reaction molecules. The rates of production and consumption were derived from a modified power-law rate expression. According to the results, the adapted rate model can deliver a better prediction of final conversion and selectivity. Therefore, the temperature dependence of the pre-exponential factor was considered explicitly due to its considerable effects on the rate of reactions. The kinetic parameters were estimated by global optimization in MATLAB using a global search method. This method was applied as an alternative to traditional (gradient-based) optimization methods to avoid convergence to the local minima during the search process. Optimum values were achieved during the search process and they were not significantly different. These values were determined within the acceptable range compared to the literature values. The modelling results were in good agreement with the experimental data. It was found that the model based on the modified equation provided a better fit to the experimental data with a mean absolute relative residual (MARR) of 6.57%, compared to the classic equation with a MARR of 12.24%.

The effects of Fischer-Tropsch, water gas shift and methanation reaction rates on CO and H_2 conversion as well as selectivity of CO_2, CH_4 C_2, C_3, C_4, and C_{5+} were investigated at 503 K, 15 bar and 6 L g_{cat}^{-1} h^{-1}. It was concluded that the conversion rates of CO and H_2 are strongly dependent on the FT reaction rates in which the conversion of 91.57 and 97.26% respectively, were achieved with the FT reaction rate of 7.81×10^{-5} mol g_{cat}^{-1} s^{-1}. The higher rate of C_{5+} formation was found with the increasing of the FT reaction rates compared to the rate of lighter hydrocarbons' formation. At the same condition, only 5.04 and 8.91% methane and C_2-C_4 selectivity were predicted while obtaining the highest value of 86.05% liquid (C_{5+}) selectivity. It was concluded that the greater rate of conversion of H_2 inside pores filled with liquid products, compared to that of CO, caused an increase in the H_2/CO ratio in the catalyst's pores; and thus, a shift towards the formation of lighter HCs. Also, the 37% Co/SiO_2 catalyst was very active due to the high percentage of cobalt content; this was one of the contributing factors to the increasing of the FT reaction rates. The FT reaction rates increase with an increase in the pore size. The catalyst with a small pore diameter exhibits low activity; a significant increase in FT reaction rates can be observed by increasing the pore size. Higher reducibility of large cobalt particles is likely to be one of the reasons for the higher FT reaction rates and lower methane selectivity on wider pore cobalt catalysts. In the present model, the CO_2 formation was non-negligible and H_2O partial pressure was identified as one of the key factors influencing the reaction rate; this led to the conclusion that the WGS reaction is responsible for this result. The best fit of the experimental data corresponded to a model postulating the irreversibility of CO_2 formation. Water was produced as the reaction occurred at the surface of the catalyst. It was shown that the production of H_2O increased by increasing the FT reaction rates; however, the rate of CO mole fraction reduction reduced by the increasing of the FT reaction rates. At some point, the rate of the H_2O formation is larger than the rate of reduction of CO mole fraction and therefore could result in a slight increase of CO_2 selectivity.

Acknowledgments

Nima Moazami would like to extend thanks for the provision of a Ph.D. scholarship to the School of Mechanical Engineering, The University of Birmingham, UK. This opportunity enables him to continue his work on the modelling of reforming and FT reactors.

Nomenclature

Symbols

a_j	pre-exponential factor of rate constant in reaction 'j', [mol $Pa^{-(m_j+n_j)}$ g_{cat}^{-1} s^{-1}]
A_r	reactor surface area, [m^2]
C_i	concentration of species 'i', [mol m^{-3}]
d_p	average particle diameter, [m]
E_j	activation energy of reaction 'j', [J mol^{-1}]
f	friction factor, [-]
k_j	rate constants, [mol $Pa^{-(m_j+n_j)}$ g_{cat}^{-1} s^{-1}]
M_i	molecular weight of species 'i', [g mol^{-1}]
M_m	molecular weight of mixture, [g mol^{-1}]
m	partial order of the reactant with respect to hydrogen, [-]
n	partial order of the reactant with respect to carbon monoxide, [-]
p_i	partial pressure of species 'i', [bar]
p_T	total pressure, [bar]
Q	volumetric flow rate of the fluid, [m^3 s^{-1}]
R_j	rate of reaction 'j', [mol g_{cat}^{-1} s^{-1}]
Re	Reynolds number, [-]
R_g	universal gas constant, 8.314 [J mol^{-1} K^{-1}]
S_i	selectivity of species 'i', [%]
T	reaction temperature, [K]
T_r	reference temperature, [K]
u_s	superficial fluid velocity, [m s^{-1}]
x	conversion, [%]

Y_i	mole fraction of species 'i', [-]

Greek letters

β	volume fraction of active site of the solid particles, [-]
δ	explicit temperature dependence factor of the pre-exponential constant, [-]
ϵ	void fraction, [-]
μ_i	dynamic viscosity of species 'i', [kg m^{-1} s^{-1}]
μ_m	dynamic viscosity of the mixture, [kg m^{-1} s^{-1}]
ρ_f	density of the fluid, [kg m^{-3}]
ρ_B	density of the bulk, [kg_{cat} m^{-3}]

Subscripts

0	initial value
i	species number
j	reaction number
m	mixture
z	axial dimension

Abbreviations

CSTR	Continuously stirred tank reactor
Co	Cobalt
FT	Fischer-Tropsch
FID	Flame Ionization detector
Fe	Iron
WHSV	Weight Hourly Space Velocity
GC	Gas Chromatogram
HC	Hydrocarbon
HCs	Hydrocarbons
MS	Mass Spectrometry
Ni	Nickel
ODEs	Ordinary differential equations
Re	Rhenium
Ru	Ruthenium
WGS	Water gas shift

References

[1] L. C. Almeida, O. Sanz, D. Merino, G. Arzamendi, L. M. Gandía, and M. Montes, "Kinetic analysis and microstructured reactors modeling for the Fischer–Tropsch synthesis over a Co–Re/Al_2O_3 catalyst," *Catalysis Today,* vol. 215, pp. 103-111, 10/15 2013.

[2] A. Haghtalab, M. Nabipoor, and S. Farzad, "Kinetic modeling of the Fischer–Tropsch synthesis in a slurry phase bubble column reactor using Langmuir–Freundlich isotherm," *Fuel Processing Technology,* vol. 104, pp. 73-79, 2012.

[3] K.-J. Woo, S.-H. Kang, S.-M. Kim, J.-W. Bae, and K.-W. Jun, "Performance of a slurry bubble column reactor for Fischer–Tropsch synthesis: determination of optimum condition," *Fuel Processing Technology,* vol. 91, pp. 434-439, 2010.

[4] J.-I. Yang, J. H. Yang, H.-J. Kim, H. Jung, D. H. Chun, and H.-T. Lee, "Highly effective cobalt catalyst for wax production in Fischer–Tropsch synthesis," *Fuel,* vol. 89, pp. 237-243, 2010.

[5] Y.-N. Wang, Y.-W. Li, L. Bai, Y.-L. Zhao, and B.-J. Zhang, "Correlation for gas–liquid equilibrium prediction in Fischer–Tropsch synthesis," *Fuel,* vol. 78, pp. 911-917, 1999.

[6] A. Steynberg and M. Dry, *Fischer-Tropsch Technology*. The Netherlands: Elsevier, 2004.

[7] I. C. Yates and C. N. Satterfield, "Intrinsic kinetics of the Fischer-Tropsch synthesis on a cobalt catalyst," *Energy & Fuels,* vol. 5, pp. 168-173, 1991.

[8] H. E. Atwood and C. O. Bennett, "Kinetics of the Fischer-Tropsch reaction over iron," *Industrial & Engineering Chemistry Process Design and Development,* vol. 18, pp. 163-170, 1979.

[9] G. Bub, M. Baerns, B. Büssemeier, and C. Frohning, "Prediction of the performance of catalytic fixed bed reactors for Fischer-Tropsch synthesis," *Chemical Engineering Science,* vol. 35, pp. 348-355, 1980.

[10] J. De Swart, "Selection, design and scale up of the Fischer-Tropsch reactor," in *Fuel and Energy Abstracts*, 1997.

[11] A. Jess, R. Popp, and K. Hedden, "Fischer–Tropsch-synthesis with nitrogen-rich syngas: fundamentals and reactor design aspects," *Applied Catalysis A: General,* vol. 186, pp. 321-342, 1999.

[12] Y.-N. Wang, W.-P. Ma, Y.-J. Lu, J. Yang, Y.-Y. Xu, H.-W. Xiang*, et al.*, "Kinetics modelling of Fischer–Tropsch synthesis over an industrial Fe–Cu–K catalyst," *Fuel,* vol. 82, pp. 195-213, 2003.

[13] R. Guettel and T. Turek, "Comparison of different reactor types for low temperature Fischer–Tropsch synthesis: a simulation study," *Chemical Engineering Science,* vol. 64, pp. 955-964, 2009.

[14] A. Jess and C. Kern, "Modeling of Multi-Tubular Reactors for Fischer-Tropsch Synthesis," *Chemical engineering & technology,* vol. 32, pp. 1164-1175, 2009.

[15] R. Philippe, M. Lacroix, L. Dreibine, C. Pham-Huu, D. Edouard, S. Savin*, et al.*, "Effect of structure and thermal properties of a Fischer–Tropsch catalyst in a fixed bed," *Catalysis Today,* vol. 147, pp. S305-S312, 2009.

[16] M. H. Rafiq, H. A. Jakobsen, R. Schmid, and J. E. Hustad, "Experimental studies and modeling of a fixed bed reactor for Fischer–Tropsch synthesis using biosyngas," *Fuel processing technology,* vol. 92, pp. 893-907, 2011.

[17] N. Park, J.-R. Kim, Y. Yoo, J. Lee, and M.-J. Park, "Modeling of a pilot-scale fixed-bed reactor for iron-based Fischer–Tropsch synthesis: Two-dimensional approach for optimal tube diameter," *Fuel,* vol. 122, pp. 229-235, 4/15/ 2014.

[18] C.-H. Yang, F. E. Massoth, and A. G. Oblad, "Kinetics of CO + H_2 Reaction over Co-Cu-Al_2O_3 Catalyst," in *Hydrocarbon Synthesis from Carbon Monoxide and Hydrogen*. vol. 178, ed: American Chemical Society, 1979, pp. 35-46.

[19] J. Wang, " Ph.D. Thesis, Bringham Young University, Provo, UT," 1987.

[20] R. Zennaro, M. Tagliabue, and C. H. Bartholomew, "Kinetics of Fischer–Tropsch synthesis on titania-supported cobalt," *Catalysis Today,* vol. 58, pp. 309-319, 2000.

[21] T. K. Das, W. A. Conner, J. Li, G. Jacobs, M. E. Dry, and B. H. Davis, "Fischer-Tropsch synthesis: kinetics and effect of water for a Co/SiO_2 catalyst," *Energy & fuels,* vol. 19, pp. 1430-1439, 2005.

[22] M. A. Marvast, M. Sohrabi, S. Zarrinpashne, and G. Baghmisheh, "Fischer-Tropsch Synthesis: Modeling and Performance Study for Fe-HZSM5 Bifunctional Catalyst," *Chemical Engineering & Technology,* vol. 28, pp. 78-86, 2005.

[23] K. Jarosch, B. Yang, S. Fitzgerald, R. Taha, T. Mazanec, and A. Tonkovich, "Preprints of Paper," *American Chemical Society, Division of Fuel Chemistry,* vol. 53, pp. 90-91, 2008.

[24] W. Ma, G. Jacobs, D. E. Sparks, M. K. Gnanamani, V. R. R. Pendyala, C. H. Yen*, et al.*, "Fischer–Tropsch synthesis: Support and cobalt cluster size effects on kinetics over Co/Al_2O_3 and Co/SiO_2 catalysts," *Fuel,* vol. 90, pp. 756-765, 2011.

[25] W. Ma, G. Jacobs, T. K. Das, C. M. Masuku, J. Kang, V. R. R. Pendyala*, et al.*, "Fischer–Tropsch Synthesis: Kinetics and Water Effect on Methane Formation over 25% Co/γ-Al_2O_3 Catalyst," *Industrial & Engineering Chemistry Research,* vol. 53, pp. 2157-2166, 2014.

[26] H. Mahmoudi, "Performance of cobalt-based eggshell catalyst in lowtemperature Fischer-Tropsch synthesis process to produce long-chain hydrocarbons from synthesis gas utilizing fixed-bed reactor technology," Ph.D. Thesis, School of Mechanical Engineering, University of Birmingham, 2015.

[27] N. Moazami, M. L. Wyszynski, H. Mahmoudi, A. Tsolakis, Z. Zou, P. Panahifar*, et al.*, "Modelling of a fixed bed reactor for Fischer–Tropsch synthesis of simulated N2-rich syngas over Co/SiO2: Hydrocarbon production," *Fuel,* vol. 154, pp. 140-151, 8/15/ 2015.

[28] A. Y. Khodakov, A. Griboval-Constant, R. Bechara, and V. L. Zholobenko, "Pore Size Effects in Fischer Tropsch Synthesis over Cobalt-Supported Mesoporous Silicas," *Journal of Catalysis,* vol. 206, pp. 230-241, 3/10/ 2002.

[29] C. G. Visconti, E. Tronconi, L. Lietti, P. Forzatti, S. Rossini, and R. Zennaro, "Detailed kinetics of the Fischer–Tropsch synthesis on cobalt catalysts based on H-assisted CO activation," *Topics in Catalysis,* vol. 54, pp. 786-800, 2011.

[30] G. F. Froment and K. B. Bischoff, *Chemical reactor analysis and design*: Wiley, 1990.

[31] N. Moazami, M. Wyszynski, and H. Mahmoudi, "Modeling of catalytic monolith reactor for reforming of hexadecane with exhaust gas," *International Journal of Hydrogen Energy,* vol. 38, pp. 11826-11839, 2013.

[32] R. E. Hayes and S. T. Kolaczkowski, *Introduction to catalytic combustion*: CRC Press, 1998.

[33] G. F. Froment, K. B. Bischoff, and J. De Wilde, *Chemical reactor analysis and design* vol. 2: Wiley New York, 1990.

[34] D. W. Green, *Perry's chemical engineers' handbook* vol. 796: McGraw-hill New York, 2008.
[35] C. L. Yaws, *Thermophysical properties of chemicals and hydrocarbons*: William Andrew, 2008.
[36] D. Song and J. Li, "Effect of catalyst pore size on the catalytic performance of silica supported cobalt Fischer–Tropsch catalysts," *Journal of Molecular Catalysis A: Chemical,* vol. 247, pp. 206-212, 3/16 2006.
[37] B. Todic, T. Bhatelia, G. F. Froment, W. Ma, G. Jacobs, B. H. Davis*, et al.*, "Kinetic Model of Fischer–Tropsch Synthesis in a Slurry Reactor on Co–Re/Al_2O_3 Catalyst," *Industrial & Engineering Chemistry Research,* vol. 52, pp. 669-679, 2013/01/16 2012.
[38] S. Storsæter, D. Chen, and A. Holmen, "Microkinetic modelling of the formation of C_1 and C_2 products in the Fischer–Tropsch synthesis over cobalt catalysts," *Surface science,* vol. 600, pp. 2051-2063, 2006.
[39] E. Iglesia, "Design, synthesis, and use of cobalt-based Fischer-Tropsch synthesis catalysts," *Applied Catalysis A: General,* vol. 161, pp. 59-78, 1997.
[40] N. Tsubaki, S. Sun, and K. Fujimoto, "Different Functions of the Noble Metals Added to Cobalt Catalysts for Fischer–Tropsch Synthesis," *Journal of Catalysis,* vol. 199, pp. 236-246, 4/25/ 2001.
[41] J. Li, X. Zhan, Y. Zhang, G. Jacobs, T. Das, and B. H. Davis, "Fischer–Tropsch synthesis: effect of water on the deactivation of Pt promoted Co/Al_2O_3 catalysts," *Applied Catalysis A: General,* vol. 228, pp. 203-212, 2002.
[42] I. Chernobaev, M. Yakubovich, A. Tripol'skii, N. Pavlenko, and V. Struzhko, "Investigation of the mechanism of methane formation in the Fischer-Tropsch synthesis on a Co/SiO_2. Zr IV catalyst," *Theoretical and Experimental Chemistry,* vol. 33, pp. 38-40, 1997.

Highlights

- Fischer–Tropsch synthesis over cobalt-silica was conducted in a fixed bed reactor.
- Conversion and production rates were correlated by modified power-law rate model.
- Reactor model and reaction kinetics were developed and fitted against experiments.
- The performance of process was examined for its potential in liquid production.
- The influence of reaction rates on syngas conversion was studied for more efficient synthesis.